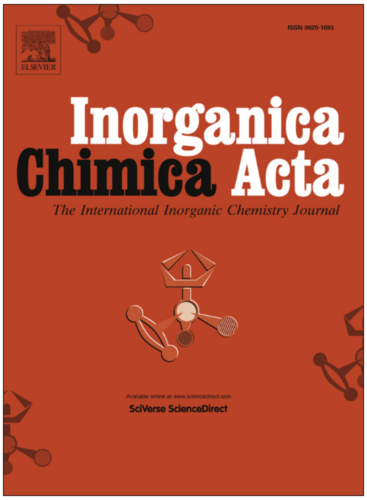

Dinuclear vanadium, copper, manganese and titanium complexes containing O,O,N-dichelating ligands: synthesis, crystal structure and catalytic activity

Hassan Hosseini-Monfared, Nasim Asghari-Lalami, Aleksandra Pazio, Krzysztof Wozniak, Christoph Janiak

PII: S0020-1693(13)00243-0
DOI: http://dx.doi.org/10.1016/j.ica.2013.04.044
Reference: ICA 15449

To appear in: *Inorganica Chimica Acta*

Received Date: 5 February 2013
Revised Date: 24 April 2013
Accepted Date: 24 April 2013

Please cite this article as: H. Hosseini-Monfared, N. Asghari-Lalami, A. Pazio, K. Wozniak, C. Janiak, Dinuclear vanadium, copper, manganese and titanium complexes containing O,O,N-dichelating ligands: synthesis, crystal structure and catalytic activity, *Inorganica Chimica Acta* (2013), doi: http://dx.doi.org/10.1016/j.ica.2013.04.044

Dinuclear vanadium, copper, manganese and titanium complexes containing O,O,N-dichelating ligands: synthesis, crystal structure and catalytic activity

Hassan Hosseini-Monfared[a,*], Nasim Asghari-Lalami[a], Aleksandra Pazio[b], Krzysztof Wozniak [b], Christoph Janiak [c]

[a] *Department of Chemistry, University of Zanjan 45195-313, Zanjan, I. R. Iran.*

Email: monfared@znu.ac.ir

[b] *Chemistry Department, University of Warsaw, Pasteura 1, 02093 Warszawa, Poland. E-mail: kwozniak@chem.uw.edu.pl*

[c] *Institut für Anorganische Chemie und Strukturchemie, Universität Düsseldorf, Universitätsstr. 1, D-40225 Düsseldorf, Germany. E-mail: janiak@uni-duesseldorf.de*

Abstract

O,O,N- or O,N-dichelating ligands, H_4L^1, H_4L^2, derived from new bis(hydroxybenzylidene)-substituted terephthalo and oxalo hydrazides were prepared and characterized by FT-IR and NMR spectroscopy (H_4L^1 = dicondensation of salicylaldehyde and terephthalic acid dihydrazide, H_4L^2= dicondensation of salicylaldehyde and oxalic acid dihydrazide). $[\{VO_2\}_2(H_2L^1)]$ (**1**), $[\{Cu(CH_3OH)\}_2(L^1)]$ (**2**), $[\{Mn(CH_3OH)\}_2(L^1)]$ (**3**) and $[TiO(H_3L^1)_2]$ (**4**) complexes of the potentially hexadentate 2[ONO] donor hydrazone ligand $[L^1]^{4-}$ were synthesized by reaction of the appropriate metal salts with H_4L^1. The complexes [{VO(CH_3O)(CH_3OH)}$_2$(L^2)] (**5**), [{Cu(CH_3OH)}$_2$(L^2)] (**6**), [{Mn(H_2O)$_2$(CH_3OH)}$_2$(L^2)] (**7**) and [{TiO(CH_3OH)}$_2$(L^2)]·2H_2O (**8**) were synthesized by the reaction of corresponding metal salts with H_4L^2. All complexes were characterized by microanalyses, FT-IR, UV–Vis and NMR spectroscopic methods. The crystal structures of **1** and **5** were established by X-ray analyses. Compound **1** is a one-dimensional coordination polymer. The catalytic potential of the complexes was evaluated for oxidation of hydrocarbons including cycloalkenes, cyclic alkanes and benzylalcohol using H_2O_2 as terminal oxidant. Of the studied aroylhydrazone complexes, **4** showed the best selectivity and activity as catalyst.

Keywords: Terephthalohydrazide; Oxalohydrazide; Transition metal; Structure; Oxidation; Hydrocarbon

1. Introduction

Coordination chemistry of aroylhydrazones has been a subject of competitive research since they exhibit a wide range of catalytic oxidation reaction properties, especially aroylhydrazones which are derived from heterocyclic aldehydes or ketones [1,2,3]. Aroylhydrazone complexes show the potential to be good oxidation catalysts because of bearing the necessary condition of stability towards oxidation. Also, the world-wide demand for valuable oxidation products that can be produced in high yields and purities grows substantially year after year [4,5]. The driving force is a strong economic incentive to find better and more cost effective catalyst systems that can produce these value added oxidation products. New catalysts can provide the potential to shift the production of expensive niche products to value added commodity products [6]. The demand for more environmentally acceptable methods in fine chemistry that allow elimination of common but otherwise hazardous or costly oxidants, such as organic peroxyacids, is pushing forward the use of cleaner oxidants like hydroperoxides (particularly hydrogen peroxide) under catalytic conditions [7,8].

Acyl- and aroylhydrazones are multipurpose class of ligands (Scheme 1) having a range of biological and chemical activities. Hydrazones exhibit physiological and biological activities in the treatment of several diseases such as tuberculosis [9], for the treatment of Fe overload disease [10,11], and as inhibitors for many enzymes [12]. Their metal complexes have also found applications in various chemical processes like non-linear optics, sensors, and medicine [13]. They are of interest in the field of electrochromism where a change in the oxidation state of the metal is possible [14]. The acyl and aroylhydrazones –CO–NH–N=CR´R´´ (R, R´, R´´=H, alkyl, aryl) contain trigonal N- and O-donor atoms that can coordinate to metal ions [15,1]. Hydrazone ligands can act as bidentate, tridentate, or tetradentate ligands depending on the nature of heterocyclic ring substituents attached to the hydrazone unit. These ligands exhibit a facile keto–enol tautomerization (Scheme 1b) which can modulate the coordination to the metal as a uni-negative or di-negative ligand in the keto or enol form, respectively (Scheme 2b). In the field of hydrazone chemistry, the study of bis(aryl)hydrazone complexes is of interest for several reasons: (1) the study of the bis(aryl)hydrazone complexes is justified by the presence of two hydrazone coordinating units in ditopic ligands, which may yield supramolecular architectures or coordination polymers [16], (2) the coordination of a metal ion by one unit may induce changes in the coordinative properties of the other unit, and (3) binuclear complexes of these ligands are suitable for weak spin–spin exchange interaction studies [17].

Herein we report the synthesis, crystal structure, spectroscopic properties and catalytic activity of terephthalo- and oxalohydrazide complexes of V(V), Cu(II), Mn(II)and Ti(IV) with 1D polymeric, dinuclear and mononuclear structures (Scheme 3).

2. Experimental

All materials with high purity were purchased from Merck and Fluka and used as received. IR spectra were recorded as KBr disks with a Matson 1000 FT-IR spectrophotometer in the range of 4000–450 cm^{-1}. UV–Vis spectra of solution were recorded on a Shimadzu 160 spectrometer. ^1H NMR spectra in DMSO-d_6 and $CDCl_3$ solution were recorded on a Bruker 250 MHz spectrometer and chemical shifts are indicated in ppm relative to tetramethylsilane. The oxidation products were determined and analyzed by a HP Agilent 6890 gas chromatograph equipped with a HP-5 capillary column (phenyl methyl siloxane 30 m long × 320 µm i.d.× 0.25 µm film thickness). The elemental analyses (carbon, hydrogen, and nitrogen) of compounds were obtained from Perkin Elmer Model 2400 analyzer. Copper, manganese, titanium and vanadium percentages of complexes were measured by a Varian spectrometer AAS-220. Electrical conductivity of complexes was measured by a Metrohm 712Conductometer with cell constant 0.8 cm^{-1}.

2.1. Synthesis of H_4L^1

2.1.1. Synthesis of diethyl terephthalate

Diethyl terephthalate was produced as reported in the literature [18]. Terephthalic acid (0.50 g, 3.0 mmol) in dry ethanol (20 mL) containing 2-3 drops of concentrated H_2SO_4 was refluxed for 24 h till it dissolved. Then the reaction mixture was poured in ice-cold water. Immediately a white solid started separating from the clear solution. Then sodium bicarbonate was used for the neutralization of excess acid. Addition of sodium bicarbonate was continued till the effervescence seized. The ester was filtered, washed several times with water, and dried in air. Yield: 84% (0.57 g). M.p. 44.5°C. ^{1}H NMR (250.13 MHz, DMSO-d_6): δ = 1.31 (t, *J* 7.0, 6H; CH_3), 4.32 (q, *J* 7.7, 4H; CH_2), 8.05 ppm (s, 4H, aryl).

2.1.2. Synthesis of terephthalohydrazide

A mixture of diethyl terephthalate (0.10 g, 0.45 mmol) and hydrazine hydrate (98%, 2 mL) in toluene (10 mL) was refluxed for 9-10 h. A white precipitate of terephthalohydrazide was formed, filtered, washed with toluene and then dried at air. Yield: 52% (45 mg). ^{1}H NMR (250.13 MHz, DMSO-d_6): δ = 4.51 (s, 4H, –NH_2), 7.83 (s, 4H, aryl), 9.86 ppm (s, 2H, –NH–). ^{13}C {^{1}H} NMR (62.89 MHz, DMSO-d_6): δ = 127.4-129.5 (4C), 135.9 (2C), 165.6 (2C, C=O).

2.1.3. Synthesis of N'^1,N'^4-bis(2-hydroxybenzylidene)terephthalohydrazide (H_4L^1)

A mixture of terephthalohydrazide (0.26 g, 0.88 mmol) and salicylaldehyde (0.216 g, 1.77 mmol) was refluxed in ethanol (10 mL) for 5 hours. The resulting yellow precipitate was filtered, washed with ethanol and dried at air. Yield: 87% (0.47 g). IR (KBr, cm^{-1}): 3443 (w, OH), 3221 (s, N-H), 3044 (m), 1655 (vs, C=O), 1640 (s, C=N), 1551 (m), 1488 (s), 1364 (s), 1287 (s), 1204 (m), 1148 (m), 1119 (m), 1081 (m), 1035 (m), 963 (m, N-N), 918 (m), 871 (s), 740 (s), 656 (s),483 (m), 439 (m). ^{1}H NMR (250.13 MHz, DMSO-d_6, ppm): δ = 6.90-8.06 (m, 12 H, aryl), 8.65 (s, 2H, C*H*=N), 11.18 (s, 2H, aryl-O*H*), 12.21 (s, 2H, N*H*). ^{13}C {^{1}H} NMR (62.89 MHz, DMSO-d_6, ppm): δ = 116.9, 119.1, 119.8, 128.3, 129.8, 132.0, 136.2 (16C, aryl rings), 149.0 (2C, *C*H=N), 157.9 (2C, *C*-OH), 162.5 (2C, *C*=O). UV–Vis (in CH_3OH, $c = 1\times10^{-5}$ mol L^{-1}, very light yellow solution, λ_{max} [nm] with ε [L mol^{-1} cm^{-1}]): 220 (53900), 301 (38500), 339 (36900).

2.2. Synthesis of H_4L^2

2.2.1. Synthesis of dimethyl oxalate

Dimethyl oxalate was synthesized according to the reported procedure [19]. Concentrated sulfuric acid (0.5 mL) was slowly added to a solution of oxalic acid (0.90 g, 10 mmol) in methanol (2 mL). The mixture was heated near to boiling point and then filtered. After a few hours, the colorless crystals of dimethyl oxalate settled down in the filtrate. They were filtered, washed with cold methanol and dried in air. Yield: 69% (0.82 g). M.p. 51°C.^{1}H NMR (250.13 MHz, DMSO-d_6): δ = 3.89ppm (s, 6H, CH_3).

2.2.2. Synthesis of oxalohydrazide

A mixture of dimethyl oxalate (0.06 g, 0.05 mmol) and hydrazine hydrate (98%, 2 mL) in methanol was refluxed for 8 h. The white precipitate of oxalohydrazide was filtered, washed with methanol and dried in air. Yield: 75% (0.045 g). ^{1}H NMR (250.13 MHz, DMSO-d_6): δ = 4.47 (s, 4H, NH_2), 9.85 (s, 2H, NH). ^{13}C{^{1}H} NMR (62.89 MHz, DMSO-d_6): δ = 158.3 (2C, C=O).

2.2.3. Synthesis of N'^1,N'^2-bis(2-hydroxybenzylidene)oxalohydrazide (H_4L^2)

Solution of oxalohydrazide (236 mg, 0.2 mmol) and salicylaldehyde (488 mg, 0.4 mmol) in methanol (10 mL) was refluxed for 10 h. A milky precipitate was formed which was filtered, washed with methanol and dried at air. Yield: 92% (60 mg). IR (KBr, cm^{-1}): 3281 (m, OH), 3210 (m, NH), 3171 (m), 3071 (m), 1667 (vs, C=O), 1604 (s, C=N), 1536 (s), 1487 (m), 1459 (m), 1361 (s), 1308 (m), 1263 (s), 1224 (m), 1163 (m), 1056 (m), 968 (m), 876 (m), 829 (s), 758 (s), 733 (m), 635 (m), 531 (m). ^{1}H NMR (250.13 MHz, DMSO-d_6): δ = 6.90-7.54 (m, 8H, aryl), 8.79 (s, 2H, C*H*=N), 10.97 (s, 2H, OH), 12.65 (s, 2H, NH). ^{13}C{^{1}H} NMR (62.89 MHz, DMSO-d_6): δ = 116.9, 119.1, 119.9, 129.8, 132.5, (10C, aryl rings), 151.4 (2C, *C*H=N), 156.3 (2C, (aryl)C-OH), 158.0 (2C, C=O). UV–Vis (in CH_3OH, $c = 1\times10^{-5}$ mol L^{-1}, very light yellow solution, λ_{max} [nm] with ε [L mol^{-1} cm^{-1}]): 214 (13100), 240 (8600), 302 (18400), 342 (18200).

2.3. Synthesis of metal complexes

General procedure: The appropriate ligand (H_4L^1 or H_4L^2) (1.0 mmol) was dissolved in methanol (10 mL). The desired metal salt (vanadium(IV) oxide acetylacetonate [$VO(acac)_2$], $Cu(OAc)_2{\cdot}H_2O$ or $Cu(NO_3)_2{\cdot}5/2H_2O$, $Mn(OAc)_2{\cdot}4H_2O$, $TiO(acac)_2$ (2.0 mmol) was added and the solution was gently refluxed for 6 h. After cooling, the resulting solid was filtered off, washed with cooled absolute methanol and then dried in air. The analytical and physical data of the complexes are given in Table 1.

2.4. X-ray structure determination

The single crystal X-ray scattered intensities of reflections were collected for **1** and **5** using a BRUKER KAPPA APEXII ULTRA controlled by APEXII [20] software, equipped with an APEX-II CCD detector and a MoKα rotating anode X-ray source (λ = 0.71073 Å, 50.0 kV, 22.0 mA) mono chromatized by multi-layer optics. Experiments were carried out at 100(2) K for a single crystal of **1** (red plate) and 90(2) K for **5** (red-brown plate) using the Oxford Cryo stream cooling device. Single crystals were mounted on a nylon loop with a droplet of Paratone-N oil and immediately cooled. Indexing, integration and initial scaling were performed with *SAINT* and *SADABS* software (Bruker, 2007). Details of data collection procedure are given in Table 2.

Both structures were solved by direct methods using the SHELXS-97 program and refined with SHELXL-97. The multi-scan absorption correction was applied in the scaling procedure.

The refinement was based on F^2 for all reflections except those with negative intensities. Weighted R factors wR and all goodness-of-fit values were based on F^2, whereas conventional R factors were based on the amplitudes, with F set to zero for negative F^2. The $F_o^2 > 2\sigma(F_o^2)$ criterion, applied only for R factors calculation, was not relevant to the choice of reflections for the refinement. The hydrogen atoms were located in idealized geometrical positions except H10 in structure **5** which was found from the residual electron density. Scattering factors were taken from Tables 4.2.6.8 and 6.1.1.4 from the International Crystallographic Tables Vol. C [20f]. All illustrations of crystal and molecular structures of **1** and **5** were drawn with DIAMOND [21].

CCDC 904953 and 904952 contains the supplementary crystallographic data for **1** and **5,** respectively. These data can be obtained free of charge from The Cambridge Crystallographic Data Centre *via* www.ccdc.cam.ac.uk/data request/cif

2.5. General oxidation procedure

The liquid phase catalytic oxidations were carried out under air (atmospheric pressure) in a 25 mL round bottom flask equipped with a magnetic stirrer and immersed in a thermostated oil bath at 80 or 60 ºC. In a typical experiment, a mixture of 30% H_2O_2 (3 mmol), solvent (3 mL), $NaHCO_3$ (0.25 mmol), chlorobenzene (0.1 g) as internal standard and cis-cyclooctene (1 mmol) was added to a flask containing the catalyst **1-8** (1.70 μmol). The course of the reaction was monitored using a gas chromatograph equipped with a capillary column and a flame ionization detector. The oxidation products were identified by comparing their retention times with those of authentic samples or alternatively by ^{1}H NMR and GC–Mass analyses. Yields based on the added substrate were determined by a calibration curve. Control reactions were carried out in the absence of catalyst, H_2O_2 and $NaHCO_3$ under the same conditions as the catalytic runs verifying that no products, or only trace yields, were detected.

3. Results and discussion

Ligands $H_4L^1$and H_4L^2 were synthesized in three-steps by a similar method. Esterification of terephthalic and oxalic acid was followed by the reaction with hydrazine hydrate to form the corresponding hydrazide. Finally the condensation reactions of hydrazide with two equivalents salicylaldehyde resulted in the formation of H_4L^1 and H_4L^2 in high yield and purity, respectively (Table 1, Scheme 2a). Ligands H_4L^1 and H_4L^2 are potentially hexadentate and could coordinate to two different metal centers by their symmetric two tridentate unites. There is a similar keto-enol tautomerism for both $H_4L^1$and H_4L^2 (Scheme 1) and their anionic forms (Scheme 2b). V(V), Cu(II), Mn(II) and Ti(IV) complexes **1**-**8** (Scheme 3) of hexadentate hydrazone Schiff base ligands were prepared by treating a methanolic solution of the ligand with two equivalents of the appropriate metal salt. Analytical and physical data of the complexes are summarized in Table 1. All complexes are binuclear except **4** which is a mononuclear complex (cf. Scheme 3).

Electrical conductivity measurements gave Λ_M values of 21–83 (Ω^{-1} cm^2 mol^{-1}) and confirmed that they are neutral and non-electrolytes [22].

^{1}H NMR data of the ligands in DMSO-d_6 confirm their proposed structure (Scheme 1). The principal peaks of the ^{1}H NMR spectra of ligands $H_4L^{1\text{-}2}$ and complexes **1**, **4**, **5**, **8** are listed in Table 3. Due to the complexity of the aromatic region (δ 8–6), no band assignments have been made for the aromatic protons. The signal at *δ* 11.41–12.21 ppm in the spectra of the ligands and complexes is assigned to the common NH-group, concomitant with the observation of a rapid loss of these signals when D_2O is added to the solution. Also the H_4L^{1-2} ligand signals between *δ* 10.97-11.18 ppm are lost upon addition of D_2O to the solution. Hence, this signal is assigned to the aromatic –OH group which is not present in **1** and **5**. The resonances in the range of *δ* from 8.65 to 8.98 ppm are assigned to the azomethine proton (–CH=N–) in the spectra of the ligands and complexes. In a study of ligands of somewhat similar type the azomethine resonance have been reported in the region *δ* 7–9 ppm [23,24].

3.1. Infrared spectra

A list of selected IR spectral data of the ligands and complexes is presented in Table 4. Appearance of N–H (3200 cm^{-1}) and C=O (about 1660 cm^{-1}) stretching vibration bands confirms the presence of the free ligands H_4L^1 and H_4L^2 in the keto form (Scheme 1). A comparison of the spectra of the complexes with the ligands provides evidence for the coordination mode of the ligands in the complexes. Presence of the ν(C=O) and ν(N–H) bands in the complexes **4** and **5** proves the coordination of H_4L^{1-2} to metal center in the keto form. Appearance of ν(C=O) in complex **5** (1670 cm^{-1}) almost at the same frequency as ligand H_4L^2 (1665 cm^{-1}) suggests that the –N-C=O bond is delocalized to a certain extent in the free and the coordinated ligand $[H_2L^2]^{2-}$. The lack of the ν(C=O) bands, present in the ligands at 1651–1665 cm^{-1}, indicates the enolization of the amide functionality upon coordination to the metal center in **2**, **3**, **6**, **7** and **8**. Instead very strong bands at ca. 1607–1622 cm^{-1} are observed, which can be attributed to the asymmetric stretching vibration of the conjugated CH=N–N=C group [25], characteristic for coordination of the enolate form of the ligands. On complexation the absence of N–H band, red shifts in azomethine (–C=N–) and carbonyl bands of the ligands show coordination of H_4L^{1-2} as tetraanionic ligand in the enol form (Scheme 1) through the deprotonated hydroxyl group ($O_{phenolate}$), azomethine nitrogen ($N_{azomethine}$) and the enol oxygen groups in the complexes **2**, **3**, **6-8** (Table 3). The shifting of the ν (C=N) stretch towards the lower wavenumbers from the free ligand also supports the coordination of azomethine nitrogen [26] to the metal. The strong ν(V=O) band around 894 and 972 cm^{-1} could be clearly identified for the complexes **1** and **5**, respectively [27].

3.2. Electronic spectra

Yellow H_4L^1 and milky H_4L^2 are soluble in polar and common organic solvents. The electronic spectra of the ligands H_4L^{1-2} in methanol show $\pi\rightarrow\pi^*$ and $n\rightarrow\pi^*$ transitions at 214-217 and 238-340 nm, respectively (Table 5). The complexes **1-8** are soluble in methanol. Table 4 provides electronic spectral data of the ligands H_4L^{1-2} and complexes along with their assignments. The electronic spectra of the complexes in CH_3OH exhibit two groups of band about 208-241 and 289-436 nm. With respect to their molar absorptivity they were assigned to $n\rightarrow\pi^*$ and $\pi\rightarrow\pi^*$ of the ligands, respectively. Electronic transitions between metal orbitals (*d-d* transitions) are covered by broad $\pi\rightarrow\pi^*$ bands and thus not observed. DFT calculations on a similar hydrazone complex showed that the LMCT transitions contribute also to the other bands [28].

With respect to microanalyses and spectral data, the formula for synthesized complexes can be summarized as in Scheme 3.

3.3. Description of the structures

The molecular structures and labeling of the atoms for the complexes **1** and **5** are displayed in Figs. 1 and 2, respectively, and selected bond lengths and angles are given in Table 6.

In the crystal lattice, the dinculear moiety $[\{VO_2\}_2(H_2L^1)]$ of compound **1** lies on a center of symmetry coinciding with the center of the C_6-terepthalate ring of $[H_2L^1]^{2-}$and, thus, one crystallographically unique vanadium atom is present. The $[H_2L^1]^{2-}$ ligand functions as a hexadentate unit to two vanadium atoms. The two dioxidovanadium(V) or $\{VO_4N\}$ chromophores in the molecular unit, together with the two monoanionic, tridentate domains of the ligand, are oriented *trans* to each other. The atoms of the $\{VO_4\}$ group are disordered over two positions (Fig. 1a). There is one major position with 76.3% occupancy and a minor site with 23.7% occupancy. In the dinuclear molecular unit, the coordination number of the vanadium atom is five due to close contacts to two oxido, a phenolate-O, imine-N and amide-O atoms with the V-O distances ranging from 1.554(6) (for V=O) to 1.933(6) Å (Table 6). This coordination number is increased to six in a distorted octahedron when one considers an additional elongated the V-O bond (2.335(6) Å) to the O4-oxido atom of the adjacent unit (Fig. 1b). This way, the dinculear units are linked into one-dimensional coordination polymeric strands. The distortion from octahedral geometry is due to the V–O–C–N–N and V–N–C–C–C–O chelate rings and a long V1---O4 bond.

Unfortunately, the charge-dictated necessary H-atom in compound **1** could not be found. Because of the disorder of the VO_3 part in this structure we also refrained from placing the H-atom at a calculated position which may have been either or both of the disordered oxygen atoms O2/O2A and O4/O4A which then become C-O2-H and V-O4(H)-V groups, respectively (cf. Fig. 1a). Formation of C-O2-H is in agreement with the C8-O2 single bond length (1.309(10) Å cf. Fig. 1a). In part, the H-atom may even be present at N2, even though from bond length arguments we suggest the presence of a C=N double bond between C8 and N2 (cf. Fig. 1a, Table 6). The problem is that both these atoms (O and N) have lone pairs of electrons so small maxima of electron density will coincide with a possible position of this hydrogen atom. In general it is difficult to discern lone-pair electron density from H-atom electron density. Hence, in summary, delocalization of the H-atom in the solid-state at least over the oxygen atoms is likely, and we prefer to leave this hydrogen position as undefined [29].

The intermolecular packing in **1** shows no significant ··· or C-H··· contacts (calculated by PLATON [30]) despite the presence of the aromatic systems in the $[H_2L^1]^{2-}$ ligand [31,32,33].

Structural analysis shows that, similar to **1**, the dinculear moiety $[\{VO(CH_3O)(CH_3OH)\}_2(L^2)]$ of compound **5** lies on a center of symmetry coinciding with the center of $[L^2]^{4-}$and, hence, one crystallographically unique vanadium atom (Fig. 2) is present. The $[L^2]^{4-}$ ligand functions as a hexadentate unit to two vanadium atoms. The two oxidovanadium(V) or $\{VO_4N\}$ chromophores in the molecular unit together with the two dianionic, tridentate domains of the ligand adopt the *trans* configuration. The vanadium atom is coordinated by the two oxygen atoms and one nitrogen atom from the $[L^2]^{4-}$ ligand, two oxygen atoms of a *cis*-positioned methanol and methoxy ligand and an oxido atom. The oxido ligand is trans to the methanol ligand. V-O distances range from 1.584 (for V=O [3]) to 2.268 Å (V---O_{CH3OH}) (Table 6). The V-O^{-} single bonds lie between 1.762 and 1.959 Å. The C-O and C-N bond lengths of amide moiety in **5** (C8-O2 1.299(8) and C8-N2 1.293(9) Å) are almost the same (Table 6). In agreement with the corresponding IR spectra. This finding also supports that the –N-C=O bond is delocalized to a certain extent in the coordinated ligand $[H_2L^2]^{2-}$ in **5**. Highest delocalization has been reported for a brown Cu-aroylhydrazone complex which shows almost the same C-O and N-C bond lengths [29]. The equal bond lengths of around 1.30 Å in the –NCO– unit in **5** agree with those in the fully deprotonated (2-oxy-3-methoxybenzylidene)benzoylhydrazide ligand in a copper complex (1.31 Å each) for which a valence structure description of $–N=C–O^{(–)} \leftrightarrow –N^{(–)}–C=O$ was assigned based on the calculated Mulliken charge densities for the amide N = –0.410 and O = –0.529 [29]. The V–O(amide) and V–O(phenolate) bond lengths for **1** and **5** are in agreement with other previously known acylhydrazone-oxidovanadium(V) complexes in the literature [2,2]. The average V=O bond length of the oxidovanadium is approximately 1.6 Å [3].

In **5** the phenyl ring C1-C6 is part of a weak ··· stacking interaction to an exactly parallel (by symmetry) counterpart with a centroid-centroid contact of 3.802(5) Å, interplanar separation of 3.476(3) Å and a slippage of 1.540 Å [31,32].

3.4. Catalytic reactivity

The catalytic oxidation of cis-cyclooctene was studied as a representative substrate with H_2O_2 in the presence of complexes **1-8**. Cis-cyclooctene oxide was the sole product. The results of control experiments revealed that the presence of catalyst and oxidant are essential for the oxidation. The oxidation of cis-cyclooctene in the absence of H_2O_2 does not occur and in the absence of catalyst the product was trace.

Bare metal M ions (M = V(IV), Cu(II), Mn(II), Ti(IV)) did not activate H_2O_2 for cis-cyclooctene oxidation (not shown in the Table). Effects of solvent, $NaHCO_3$ concentration as co-catalyst, the ratio of oxidant/substrate and the temperature were studied in order to find suitable reaction conditions to achieve the maximum conversion of cis-cyclooctene. The presence of a hydrogen peroxide activator $NaHCO_3$ with the catalysts **2**, **4** and **8** increased the catalysts activity but it did not affect the activity of the other catalysts. Fig. 3 illustrates the influence of solvent in the catalytic epoxidation of cis-cyclooctene by **1**. Methanol, ethanol, acetonitrile, chloroform and dichloromethane were tried as solvent. The highest conversion, 85% after 3 hrs, was obtained in acetonitrile. The catalytic activity of all four complexes decreased in order acetonitrile (relative dielectric constants [34], $\varepsilon/\varepsilon_0 = 37.5$) > methanol (32.7) > ethanol (26.6) > chloroform (4.9) ~dichloromethane. Overall, reactivity of the catalysts in other solvents was much lower than in acetonitrile. The catalytic activities of **1–8** were examined in oxidation of various hydrocarbons under the optimized conditions and the results are shown in Table 8. The oxidation was not achieved by **3**, **6** and **7** because of fast hydrogen peroxide decomposition by these complexes. The decomposition of hydrogen peroxide is an activated process. The presence of catalysts such as the Schiff base complexes of transition metal ions is effective in catalyzing the decomposition of hydrogen peroxide.

In the decomposition of hydrogen peroxide, the formation of HOO^{-} ions has been proposed, which is subsequently consumed through the formation of a peroxido-metal adduct. Finally, the adduct is decomposed to form dioxygen by reaction with hydrogen ions generated in the first step [35]. The effect of various transition metal ions on the decomposition of H_2O_2 has been studied and it was found that the complexes of Cu(II) ions were more active in comparison to Co(II) and Ni(II) ions [36]. Many manganese catalysts are also known to be particularly effective in the decomposition of H_2O_2 [37]. H_2O_2 dismutation by the manganese and copper complexes **3**, **6** and **7** was fast during the reaction and evolution of O_2 gas bubbles were clearly seen. However, cis-cyclooctene epoxidation was successfully catalyzed by the complexes **3**, **6** and **7** when H_2O_2 was replaced by tert-butyl hydroperoxide (TBHP) which resulted after 24 hrs in 74, 60 and 51% conversion, respectively.

Results of the oxidation of various substrates with complexes **1**, **2**, **4**, **5** and **8** under optimum conditions are summarized in Table 7. These catalysts were able to oxidize various substrates including cycloalkenes (cis-cyclooctene 60-96% conversion, cyclohexene 73-96% conversion), cycloalkanes (cyclooctane 18-50% conversion, cyclohexane 14-93% conversion) and benzyl alcohol (16-59% conversion) with aqueous 30% hydrogen peroxide. While conversion percent of the various substrates and products selectivities was different for different catalysts, the products were the same. The catalyst **4** showed the highest activity in the oxidation of cycloalkenes and cycloalkanes.

Cis-cyclooctene was converted to the corresponding epoxide with 100% selectivity. For cyclohexene in addition to cyclohexene oxide, allylic oxidation products

(2-cyclohexene-1-ol and 2-cyclohexene-1-one) were formed. Allylic oxidation has been reported by the metalloporphyrin systems in the oxidation of alkenes such as cyclohexene and is due to the radical nature of the active oxidizing species [3]. Oxidation of benzyl alcohol to benzaldehyde was investigated and medium conversions (16-59 %) were obtained. In the oxidation of cyclohexane the only product was cyclohexanol but oxidation of cyclooctane resulted in cyclooctanol and cyclooctanone.

Catalytic activities of five catalysts **1**, **2**, **4**, **5**, **8** are compared in Fig. 4. There is no single trend in the catalysts activities toward different hydrocarbons. The catalyst **4** showed the highest activity in the oxidation of cis-cyclooctene, cyclohexene and cyclohexane.

All of the studied catalysts, **1**, **2**, **4**, **5**, **8**, showed high selectivity in the oxidation of cyclohexane. The oxidation of cyclohexane under mild conditions is a topic of great interest [38]. In the literature better results have been reported by Shul'pin et al. [39] using a binuclear manganese(IV) complex ($[LMn^{IV}(O)_3Mn^{IV}L]^{2+}$, L: 1,4,7-trimethyl-1,4,7-triazacyclononane) as catalyst, in the presence of acetic acid that prevents the decomposition of H_2O_2 to water and dioxygen. However, the selectivity of manganese(IV) complexes is not comparable with **4** (Tables 7,8). Furthermore, various V(IV)/V(V)-catalysts have been used for the oxidation of cis-cyclooctene and cyclohexene with H_2O_2 and TBHP (Table 8), yet none of the reported catalysts show such high activity and/or selectivity as **1** and **5** complexes.

Table 8

Oxidation characteristics of cis-cyclooctene and cyclohexane by different transition metal complexes

Ref.	TOF (h^{-1})	Oxidant/Catalyst	Time (h)	Selec. (%)	Conv. (%)	Substrate to product	No.
This work	108	$H_2O_2/[\{VO_2\}_2(H_2L^1)]$	5	100	92	Cis-cyclooctene to cyclooctene oxide	1
This work	102	$H_2O_2/[\{VO(CH_3O)(CH_3OH)\}_2(L^2)]$	4	100	70		2
[40]	7	$TBHP/V^{IV}O(L^3)_2$ [a]	4.5	100	84		3
[41]	5	$H_2O_2/[V^VOL^4Cl]$ [b]	6	100	29		4
[41]	7	$H_2O_2/[V^VOL^5Cl]$ [c]	6	100	39		5
This work	137	$H_2O_2/NaHCO_3/[TiO(H_3L^1)_2]$	4	100	93	Cyclohexane to cyclohexanol (A) / cyclohexanone (K)	6
[42]	640	H_2O_2/acetic acid/ $[(Me_3tacn)Mn(O)_3Mn(Me_3tacn)](PF_6)_2$ [d]	1	58% A 42% K	31		7
[43]	53	$H_2O_2/MnSO_4/Me_3tacn$/Na-oxalate [d]	3	23% A 77% K	73		8
[44]	74-222	H_2O_2/acetic acid/$[LMn(\mu\text{-}O)_3MnL][PF_6]_2$ [d]	1.5-4.5	22% A 66% K	82		9

[a] TBHP = tert-butylhydroperoxide, L^3 = N-salicylidin-2-chloroethylimine

[b] $L^4 = Me_2NCH_2CH_2N(CH_2\text{-}2\text{-}O\text{-}3,5\text{-}C_6H_2{}^tBu_2)_2$

[c] $L^5 = Me_2NCH_2CH(CH_3)N(CH_2\text{-}2\text{-}O\text{-}3,5\text{-}C_6H_2{}^tBu_2)_2$

[d] L = Me_3tacn =1,4,7-trimethyl-1,4,7-triazacyclononane

4. Conclusion

Eight new complexes of V(V), Cu(II), Mn(II) and Ti(IV) were prepared and characterized and crystal structures of two V(V)complexes were determined. Bis(2-hydroxybenzylidene)terephthalohydrazide complex of V(V) forms 1D coordination polymer in the solid state. It was demonstrated that these binuclear hydrazone Schiff base complexes are active and selective catalysts for oxidation of various hydrocarbons by environmentally benign and clean oxidant H_2O_2 under mild conditions. Of the studied aroylhydrazone complexes, $[TiO(H_3L^1)_2]$ (**4**) showed the best selectivity and activity as catalyst.

Acknowledgments

The authors are grateful to the University of Zanjan, University of Warsaw and DFG grant Ja466/23-1 (for CJ and HHM) for financial assistance.

References

---

[1] O. Pouralimardan, A.C. Chamayou, C. Janiak, H. Hosseini-Monfared, Inorg. Chim. Acta 360 (2007) 1599–1608.

[2] H. Hosseini-Monfared, S. Alavi, A. Farrokhi, M. Vahedpour, P. Mayer, Polyhedron 30 (2011) 1842–1848.

[3] H. Hosseini-Monfared, S. Kheirabadi, N. Asghari-Lalami, P. Mayer, Polyhedron 30 (2011) 1375-1384.

[4] R. A. Sheldon, J. K. Kochi, Metal Catalyzed Oxidations of Organic Compounds, Academic Press, New York, 1981.

[5] T. Punniyamurthy, S. Velusamy, J. Iqbal, Chem. Rev. 105 (2005) 2329-2364.

[6] R. Schmidt, M.B. Welch, R.D. Knudsen, S. Gottfried, H.G. Alt, J. Mol. Catal. A: Chem. 222 (2004) 17–25.

[7] G. Strukul (Ed.), “Catalytic Oxidations with Hydrogen Peroxide as Oxidant.” Kluwer, Dordrecht, 1992.

[8] R.A. Sheldon, Top. Curr. Chem. 164 (1993) 21-43.

[9] M. Mohan, M.P. Gupta, L. Chandra, N.K. Jha, Inorg. Chim. Acta 151 (1988) 61–68.

[10] D.R. Richardson, P. Ponka, Am. J. Hematol. 58 (1988) 299–305.

[11] D.S. Kalinowski, P.C. Sharpe, P.V. Bernhardt, D.R. Richardson, J. Med. Chem. 51 (2008) 331–344.

[12] G. Tamasi, L. Chiasserini, L. Savini, A. Sega, R. Cini, J. Inorg. Biochem. 99 (2005) 1347–1359.

[13] M. Bakir, I. Hassan, T. Johnson, O. Brown, O. Green, C. Gyles, M.D. Coley, J. Mol. Struct. 688 (2004) 213–222.

[14] M.D. Ward, J. Solid State Electrochem. 9 (2005) 778–787.

---

[15] A.M. Stadler, J. Harrowfield, Inorg. Chim. Acta 362 (2009) 4298–4314.

[16] H. Adams, D.E. Fenton, G. Minardi, E. Mura, A.M. Pistuddi, C. Solinas, Inorg. Chem. Commun. 3 (2000) 24–28.

[17] G.M. Larin, V.V. Minin, V.F. Shul'gin, Russ. Chem. Rev. 77 (2008) 451–465.

[18] P.G. Avaji, C.H. Vinod Kumar, S.A. Patil, K.N. Shivananda, C. Nagaraju, Eur. J. Med. Chem. 44 (2009) 3552-3559.

[19] E. Bowden, Organic Syntheses, Coll. 2 (1943) 414-415.

[20] (a) APEXII-2008v1.0 BrukerNonius 2007 (b) SAINT V7.34A Bruker Nonius 2007 (c) SADABS-2004/1 BrukerNonius area detector scaling and absorption correction, **2007** (d) G.M. Sheldrick, Acta Crystallogr. A46 (1990) 467-473; (e) G.M. Sheldrick, SHELXL 93. Program for the Refinement of Crystal Structures., Univ. of Göttingen, Germany (f) International Tables for Crystallography, Ed. A., J. C. Wilson, Kluwer: Dordrecht, 1992, Vol. C.

[21] K. Brandenburg, Diamond (Version 3.2d), Crystal and Molecular Structure Visualization, Crystal Impact – K. Brandenburg & H. PutzGbr, Bonn (Germany), 2009.

[22] G.S. Girolami, T.B. Rauchfuss, R.J. Angelici, Synthesis and Technique in Inorganic Chemistry, third ed., University Science Books, Sausalito, 1999, p. 254.

[23] R.M. Silverstein, F.X. Webster, Spectroscopic Identification of Organic Compounds, sixth ed., Wiley, New York, 1998, p. 101.

[24] B. Chiswell, J.P. Crawford, E.J. O'reilly, Inorg. Chim. Acta 40 (1980) 223-228.

[25] T. Ghosh, B. Mondal, T. Ghosh, M. Sutradhar, G. Mukherjee, M.G.B. Drew, Inorg. Chim. Acta 360 (2007) 1753-1761.

[26] B. Mondal, M.G.B. Drew, T. Ghosh, Inorg. Chim. Acta 363 (2010) 2296–2306.

[27] H. Hosseini-Monfared, R. Bikas, P. Mayer, Inorg. Chim. Acta 363 (2010) 2574-2583.

[28] H. Hosseini-Monfared, S. Alavi, R. Bikas, M. Vahedpour, P. Mayer, Polyhedron 29 (2010) 3355-3362.

[29] H. Hosseini-Monfared, M. Vahedpour, M. Mahdavi Yeganeh, M. Ghorbanloo, P. Mayer, C. Janiak, Dalton Trans. 40 (2011) 1286-1294.

[30] A.L. Spek, Acta Crystallogr. D65 (2009) 148-155.

---

[31] C. Janiak, J. Chem. Soc. Dalton Trans. (2000) 3885-3896.

[32] X.J. Yang, F. Drepper, B. Wu, W.H. Sun, W. Haehnel, C. Janiak, Dalton Trans. (2005) 256-267, and supplementary material therein.

[33] M. Nishio, CrystEngComm 6 (2004) 130-158.

[34] Y. Marcus, J. Rydberg, C. Musikas, G.R. Choppin (Eds.), Principles and Practices of Solvent Extraction, Marcel Dekker, New York, 1992, p. 23.

[35] K.C. Gupta, A. K. Sutar, Coord. Chem. Rev. 252 (2008) 1420–1450.

[36] A.P. Deshmukh, V.G. Akerkar, M.M. Salunkhe, J. Mol. Catal. A: Chem. 153 (2000) 75-82.

[37] J. Brinksma, L. Schmieder, G.V. Vliet, R. Boaron, R. Hage, D.E. De Vos, P.L. Alsters, B.L. Feringa, Tetrahedron Lett. 43 (2002) 2619–2622.

[38] U. Schuchardt, D. Cardoso, R. Sercheli, R. Pereira, R.S. da Cruz, M.C. Guerreiro, D. Mandelli, E.V. Spinacé, E.L. Pires, Applied Catalysis A: General 211 (2001) 1–17.

[39] G.B. Shul'pin, G. Süss-Fink, J.R.L. Smith, Tetrahedron 55 (1999) 5345-5358.

[40] G. Grivani, G. Bruno, H. Amiri Rudbari, A. Dehno Khalaji, P. Pourteimouri, Inorg. Chem. Commun. 18 (2012) 15-20.

[41] F. Madeira, S. Barroso, S. Namorado, P.M. Reis, B. Royo, A.M. Martins, Inorg. Chim. Acta 383 (2012) 152-156.

[42] J.R. Lindsay Smith, G.B. Shul'pin, Tetrahedron Lett. 39 (1998) 4909.-4912.

[43] J.Y. Ryu, S.O. Kim, W. Nam, S. Heo, J. Kim, Bull. Kor. Chem. Soc. 24 (2003) 1835-1837.

[44] D. Veghini, M. Bosch, F. Fischer, C. Falco, Catal. Commun. 10 (2008) 347–350.

Scheme / Figure / Table captions

Scheme 1. (a) Acyl- and aroylhydrazones general formula, (b) keto–enol tautomerization in H_4L^1 and H_4L^2

Scheme 2. (a) The ligand H_4L^1synthesis and (b) deprotonation of H_4L^2 relevant to the complex formation form of $[H_2L^2]^{2-}$ and $[L^2]^{4-}$ within the tautomeric equilibrium with CH_3OH/CH_3O^- in **5**.

Scheme 3. Molecular structural formula of synthesized complexes.

Fig. 1. (a) Asymmetric unit of compound **1** with atom numbering scheme (50% ADPs); the major conformer (68.4% occupancy) of the disordered $\{VO_4\}$ group is shown with the solid ellipsoids and bonds, the minor conformer (31.6% occupancy) in the transparent mode and with 'A' atom labels. The bond lengths and valence angles are given in Table 6. (b) Polymeric strands in **1** through connection of the dinuclear molecular units by elongated (dashed) V1---O4 bonds; only the major conformer is shown; symmetry transformations *i* = –*x*, 1–*y*, 1–*z*; *ii* = –*x*, 2–*y*, 2–*z*.

Fig. 2. Dinculear molecular structure of **5** (50% thermal ellipsoids). Bond lengths and angles are given in Table 6; symmetry transformation i = 0.5–x, 0.5–y, 1–z. The L^2-ligand in **5** is part of a protic equilibrium between mostly $[L^2]^{4-}$but also some $[H_2L^2]^{2-}$ (Scheme 2).

Fig. 3. Influence of solvent in the catalytic epoxidation of cyclooctene by **1.**

Reaction conditions: catalyst **1** 1.70 µmol, cyclooctene 1.0 mmol, H_2O_2 3.0 mmol, internal standard (chlorobenzene) 0.1 g, solvent 3.0 mL.

Fig 4. Activities of the catalysts **1**, **2**, **4**, **5** and **8** in the oxidation of various substrates with H_2O_2.

Table 1

Analytical and physical data of the complexes

Table 2

Crystal data and structure refinement for **1** and **5**.

Table 3

^{1}H-NMR data of the ligands H_4L^{1-2} and complexes in DMSO-d_6

Table 4

Selected characteristic IR bands of the ligands H_4L^{1-2} and complexes

Table 5

Electronic transitionsof the ligands H_4L^{1-2} and their complexes **1-8** in methanol

---

Table 6. Selected bond distances (Å) and angles (deg) for complexes **1** and **5**.

Table 7

Oxidation of various hydrocarbons with **1**, **2**, **4**, **5**, **8** using H_2O_2 in acetonitrile.[a]

Table 8

Oxidation characteristics of cyclooctene and cyclohexane by different transition metal complexes

(a)

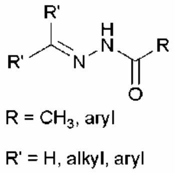
R'
H
N
N
R'
R
O
R = CH3, aryl
R' = H, alkyl, aryl

(b)

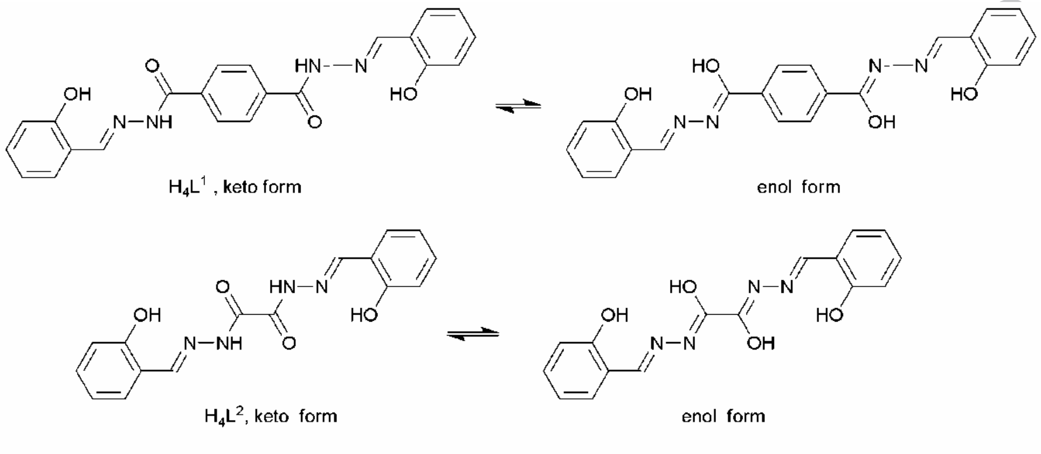
OH
N−NH
O
O
HN−−N
HO
H4L1 , keto form
HO
OH
N−N
N−−N
HO
OH
enol form
OH
N−NH
O
O
HN−N
HO
H4L2, keto form
HO
OH
N−N
N−N
HO
OH
enol form

Scheme 1

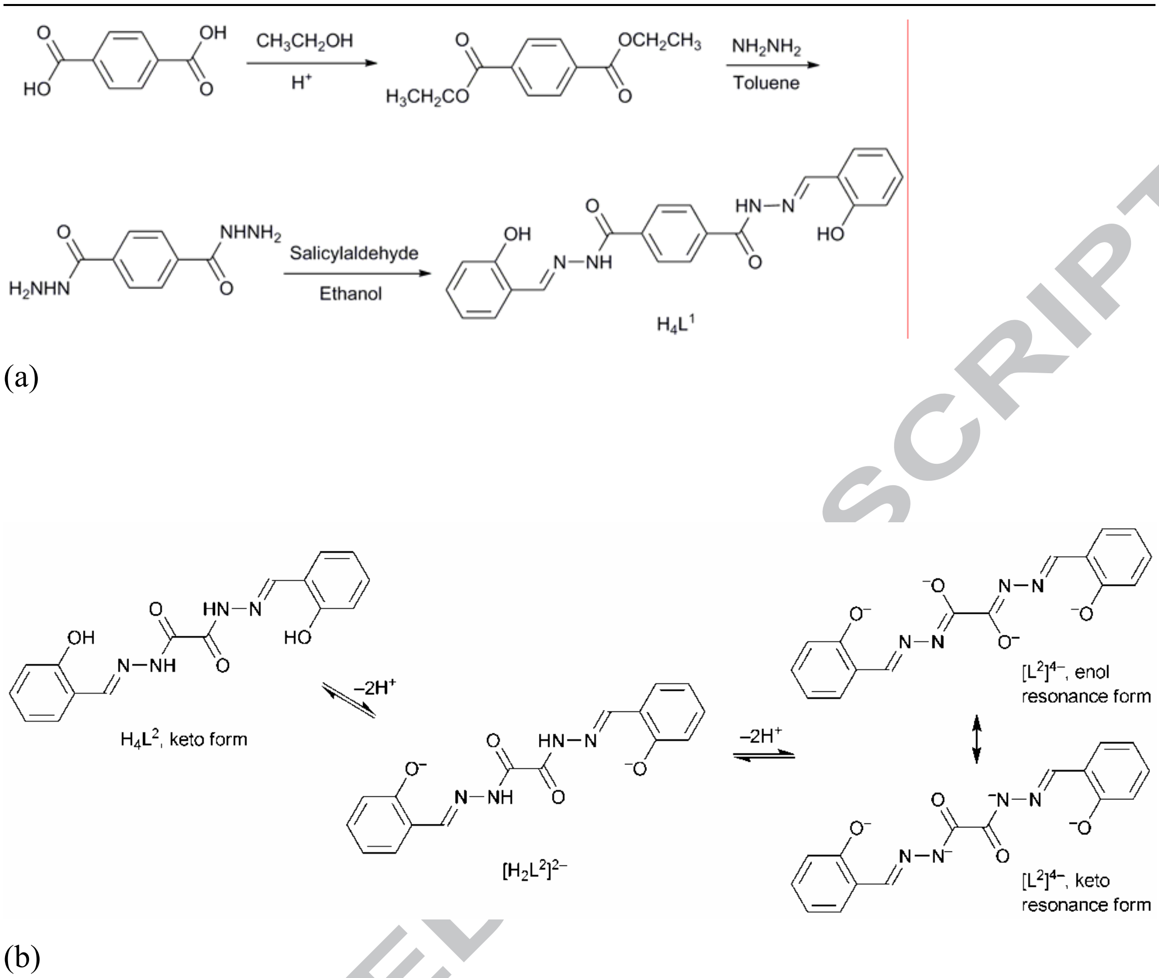
CH3CH2OH
H+
OCH2CH3
H3CH2CO
NH2NH2
Toluene
NHNH2
H2NHN
Salicylaldehyde
Ethanol
H4L1
(a)
H4L2, keto form
−2H+
[H2L2]2−
−2H+
[L2]4−, enol resonance form
[L2]4−, keto resonance form
(b)

Scheme 2

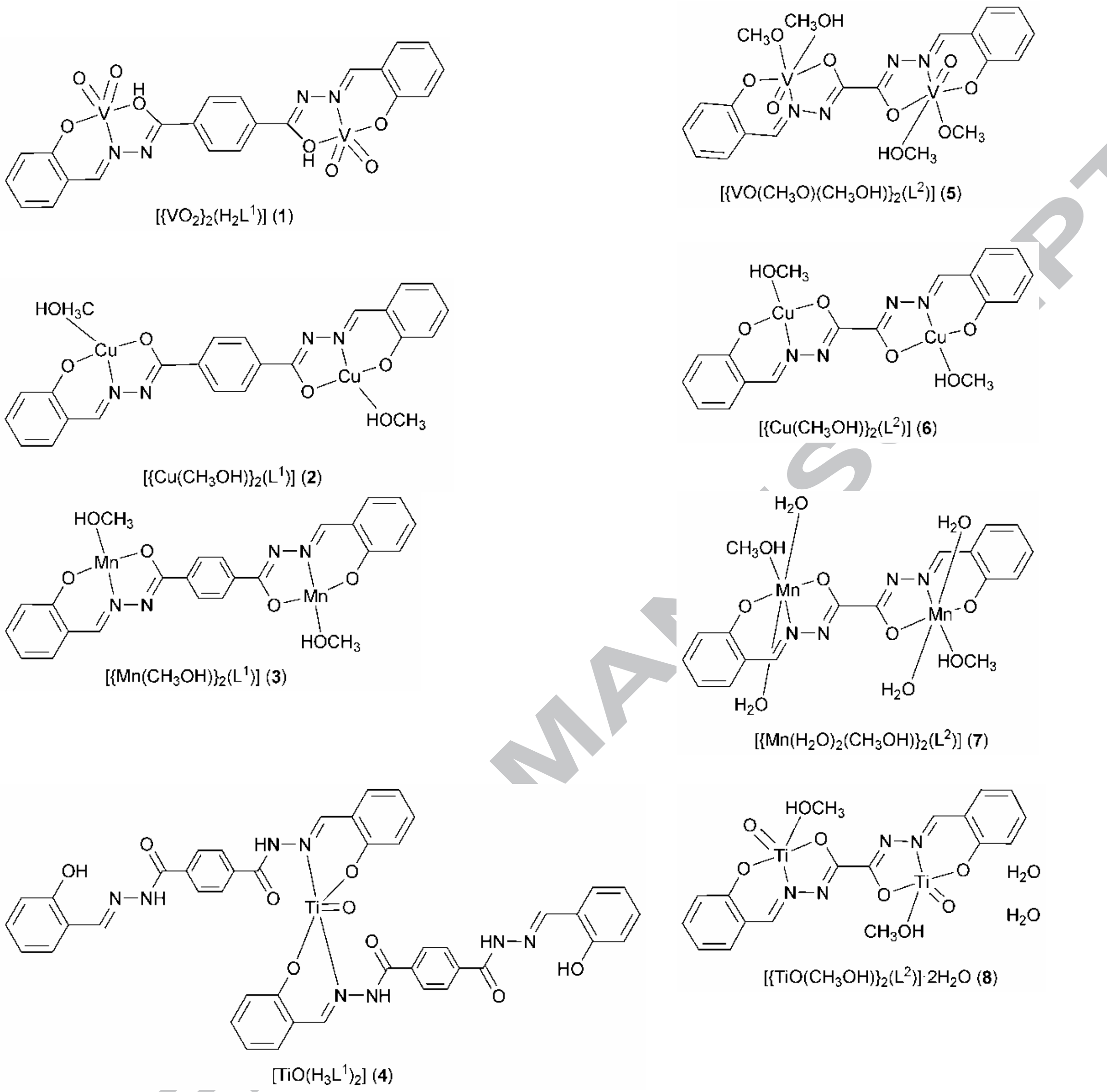

$[\{VO_2\}_2(H_2L^1)]$ (**1**)

$[\{Cu(CH_3OH)\}_2(L^1)]$ (**2**)

$[\{Mn(CH_3OH)\}_2(L^1)]$ (**3**)

$[TiO(H_3L^1)_2]$ (**4**)

$[\{VO(CH_3O)(CH_3OH)\}_2(L^2)]$ (**5**)

$[\{Cu(CH_3OH)\}_2(L^2)]$ (**6**)

$[\{Mn(H_2O)_2(CH_3OH)\}_2(L^2)]$ (**7**)

$[\{TiO(CH_3OH)\}_2(L^2)]\cdot 2H_2O$ (**8**)

Scheme 3

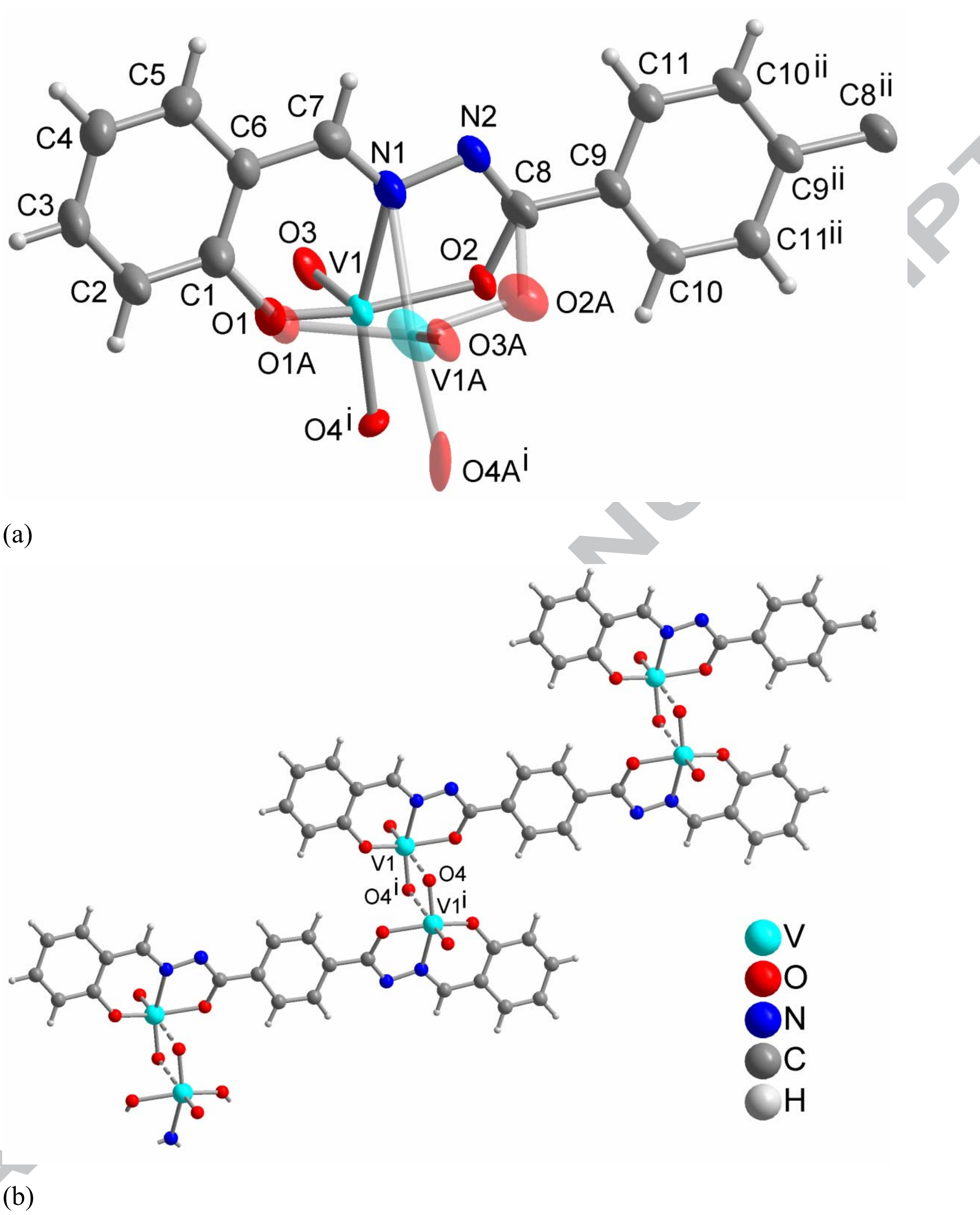
C5
C4
C3
C2
C1
C6
C7
N1
N2
C8
C9
C11
C10^{ii}
C8^{ii}
C9^{ii}
C11^{ii}
C10
O3
V1
O2
O2A
O1
O1A
O3A
V1A
O4^{i}
O4A^{i}
(a)
V1
O4^{i}
O4
V1^{i}
V
O
N
C
H
(b)

Fig. 1

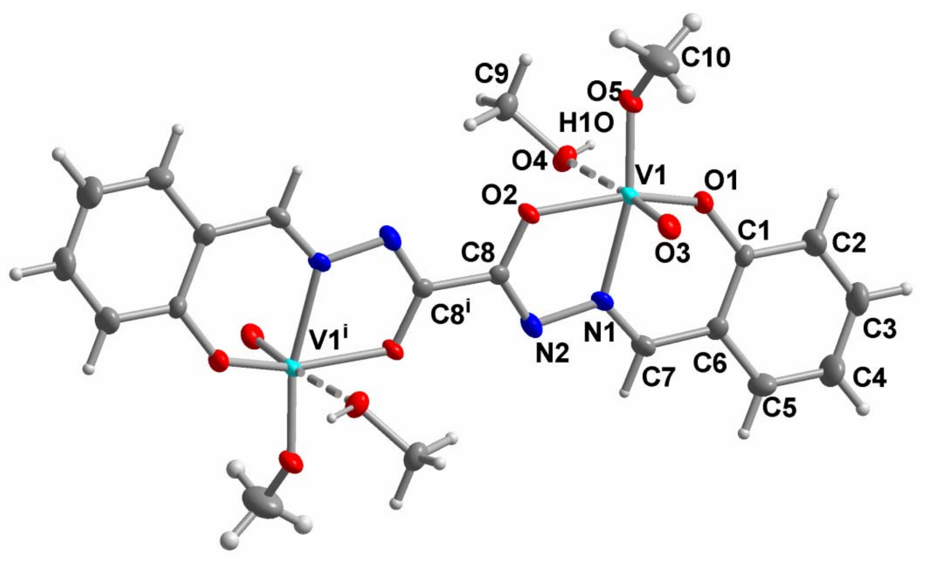
C10
C9
O5
H1O
O4
V1
O1
O2
C8
O3
C1
C2
C8^i
V1^i
N2
N1
C3
C6
C7
C5
C4

Fig. 2

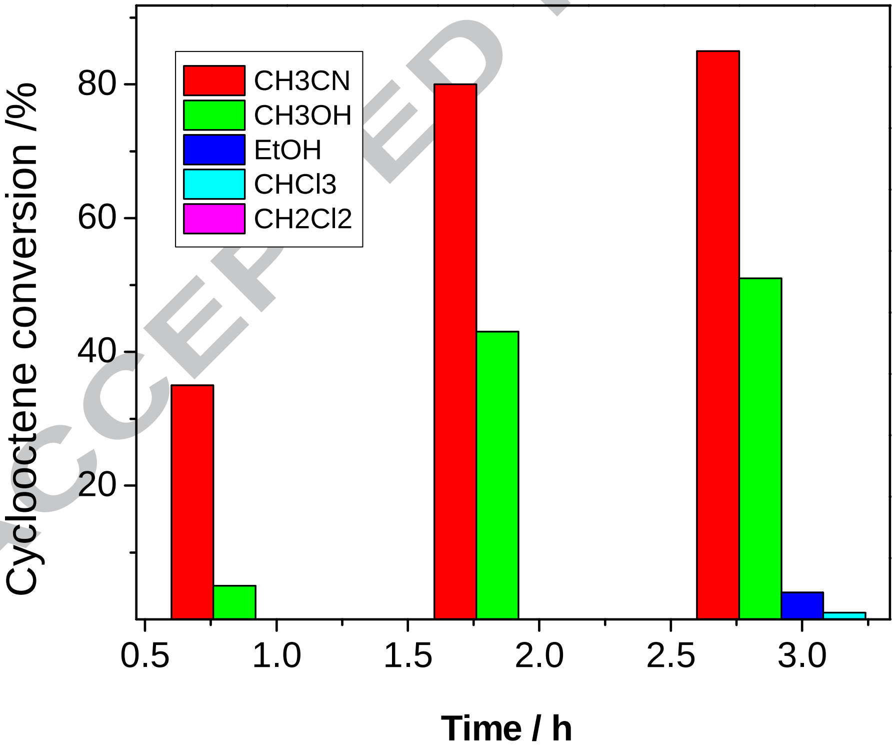
CH3CN
CH3OH
EtOH
CHCl3
CH2Cl2
Cyclooctene conversion /%
80
60
40
20
0.5
1.0
1.5
2.0
2.5
3.0
Time / h

Fig. 3

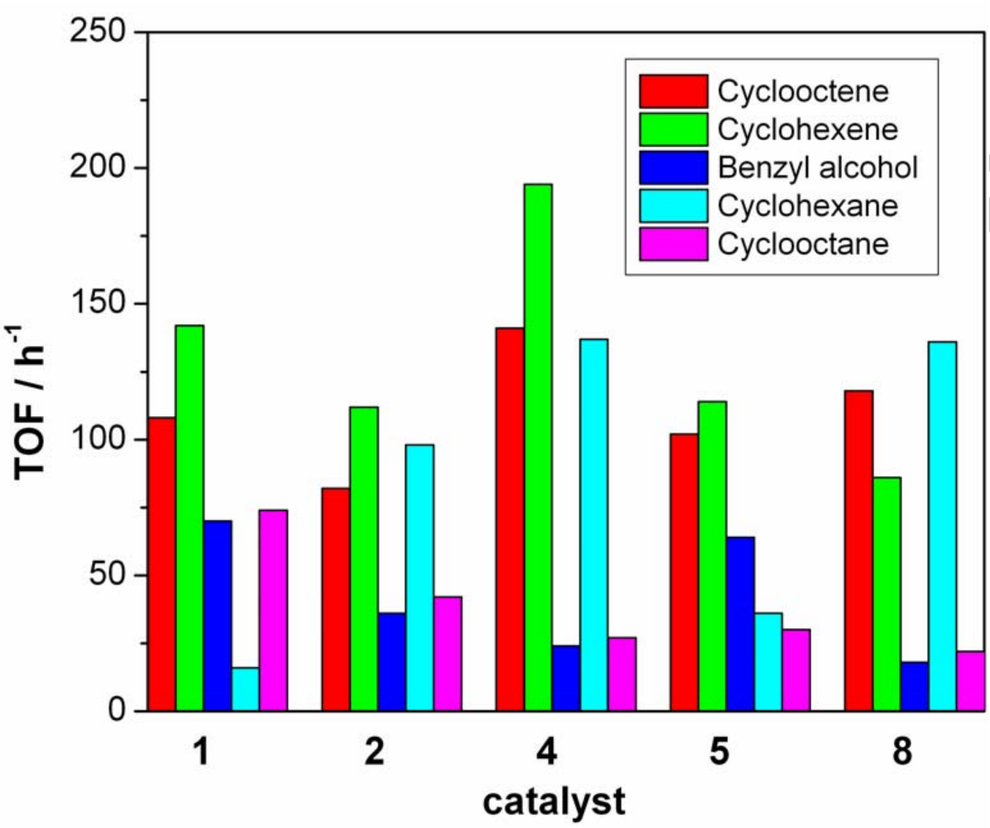

Fig 4

Table 1

Analytical and physical data of the ligands and complexes

Compound	Empirical formula (formula weight)	Yield (%)	Color	Molar conductivity (Ω^{-1} cm^2 mol^{-1})	Analyses found (Calc.) (%)			
					C	H	N	Metal
H_4L^1	$C_{22}H_{18}N_4O_4$ (MW=402.40)	87	yellow		65.64 (65.66)	4.50 (4.51)	13.96 (13.92)	
H_4L^2	$C_{16}H_{14}N_4O_4$ (MW=326.31)	92	milky		58.90 (58.89)	4.35 (4.32)	17.15 (17.17)	
1 [a]	$C_{22}H_{16}N_4O_8V_2$ (MW=566.27)	65	dark red	82.58	44.27 (46.66)	2.74 (2.85)	8.71 (9.89)	16.86 (17.99)

2	$C_{24}H_{22}N_4O_6Cu_2$ (MW=589.55)	72	green	22.77	48.76 (48.89)	2.66 (3.76)	9.95 (9.50)	20.91 (21.56)
3	$C_{24}H_{22}N_4O_6Mn_2$ (MW=572.33)	58	brown	61.82	50.81 (50.37)	4.41 (3.87)	9.25 (9.79)	19.00 (19.20)
4	$C_{44}H_{34}N_8O_9Ti$ (MW=866.66)	63	orange	56.10	60.55 (60.98)	3.65 (3.95)	12.61 (12.93)	4.95 (5.52)
5 [a]	$C_{20}H_{24}N_4O_{10}V_2$ (MW = 582.31)	83	red-brown	75.86	C 44.52 (41.25)	3.49 (4.15)	7.74 (9.62)	20.34 (17.50)
6	$C_{18}H_{18}N_4O_6Cu_2$ (MW=513.45)	75	green	33.89	46.41 (42.11)	2.97 (3.53)	10.48 (10.91)	24.43 (24.75)
7	$C_{18}H_{26}N_4O_6Mn_2$ (MW= 568.30)	74	brown	21.08	38.75 (38.04)	3.71 (4.61)	9.63 (9.86)	21.26 (19.33)
8 [a]	$C_{18}H_{22}N_4O_{10}Ti_2$ (MW= 550.12)	86	orange	49.17	37.22 (39.30)	3.45 (4.03)	10.79 (10.18)	20.05 (17.40)

[a] These compounds are found highly hygroscopic which made it difficult to exclude water adsorption during weighing for CHN and AAS sample preparation. Addition of 2 H_2O molecules per empirical formula unit of **1**, **5** and **8** accounts for the lower found C, N and M percentage.

Table 2

Crystal data and structure refinement for **1** and **5**..

Complex	**1**	**5**
Formula	$[\{VO_2\}_2(H_2L^1)]$	$[\{VO(CH_3OH)(CH_3O)\}_2(L^2)]$
Mr/g mol^{-1}	566.27	582.31
Crystal system	triclinic	monoclinic
Space group	P -1	C 2/c
a/Å	7.3988(6)	27.1940(18)
b/Å	9.2325(8)	8.3886(6)
c/Å	9.3693(8)	11.2540(7)
α/°	104.049(4)	90
β/°	100.935(5)	111.348(4)
γ/°	99.118(5)	90
V/Å^3	595.38(9)	2391.1(3)
Z, F(000)	1, 286	4, 1192
D_{calc}/g cm^{-3}	1.579	1.618
Crystal size /mm	0.34, 0.15, 0.12	0.35, 0.09, 0.05
μ/mm^{-1}	0.840	0.844
Absorption correction	Multi-Scan	Multi-Scan
Transmission factor range	0.8103-0.9462	0.852-1.000
Mean σ(I)/I	0.0292	0.0496
h; k; l range	±8; ±10; 0,11	-32, 30; 0, 9; 0, 13
θ $_{range}$	2.31-25.00	2.56-25.00
observed refls	2083	2094
x, y (weighting scheme)	0.1253, 3.0059	0.0735, 51.8930
Hydrogen refinement	Constr.	Mixed.
Refls in refinement	2083	2094

Parameters	197	170
Restraints	0	7
$R(F_{\mathrm{obs}})$ $[I > 2\ (I)]$	0.0896	0.0917
$R_{\mathrm{w}}(F^2)$ (all data)	0.2631	0.2035
Goodness-of-fit	1.124	1.083
Shift/error$_{\mathrm{max}}$	0.000	0.000
Max/min electron density/eÅ^{-3}	1.749 /-0.486	2.088/-0.461

Table 3

^{1}H-NMR data of the ligands $H_4L^{1\text{-}2}$ and complexes in DMSO-d$_6$

Compound	–C*H*=N–	–O*H*	–N*H*–
H_4L^1	8.65	11.18	12.21
H_4L^2	8.79	10.97	12.65
1	9.18	–	12.01
4	8.67	11.19	12.21
5	8.73	–	11.41
8	8.98	11.12	–

Table 4

Selected characteristic IR bands of the ligands $H_4L^{1\text{-}2}$ and complexes

Compound	ν (O–H)	ν (N–H)	ν (C=O)	ν (C=N) or ν (C=N-N=C)	
H_4L^1	3430 (w)	3213 (s)	1651 (vs)	1620 (s)	
H_4L^2	3281 (s)	3203 (m)	1665 (vs)	1604 (s)	
1	3425 (s)	-	–	1607 (vs)	894 (s, V=O)
2	3421 (m)	–	–	1617 (vs	
3	3429 (s)	–	–	1603 (vs	
4	3427 (m)	3213 (s)	1651 (vs)	1606 (vs)	
5	3423 (s)	3207 (m)	1670 (w)	1604 (vs)	972 (s, V=O)
6	3437 (s)	–	–	1613 (vs)	
7	3405 (s)	–	–	1611 (vs	
8	3427 (vs)	–	–	1622 (vs)	

Table 5
Electronic transitionsof the ligands $H_4L^{1\text{-}2}$and their complexes **1-8** in methanol.

	λ_{max}, nm (ε, L mol^{-1} cm^{-1})	
	$\pi\rightarrow\pi^*$	$n\rightarrow\pi^*$
H_4L^1	217 (53900)	300 (38500), 334 (36900)
H_4L^2	214 (13100)	238 (8600), 300 (18400), 340 (18200)
1	219(26000)	292 (25800), 353 (24000)
2	208 (7224)	416 (7965)
3	238 (48300)	332 (43300), 417 (26800)
4	223(10000)	301 (51400), 335 (53600)
5	241 (25300)	315 (16500), 399 (7300)
6	222(10200)	436 (3000)
7	213 (17431)	293 (6462), 418 (3276)
8	210 (10958)	289 (8699), 351 (6667)

Table 6. Selected bond distances (Å) and angles (deg) for complexes **1** and **5**.

	Complex **1**	Complex **5**	
V1-O1	1.835(8)	V1-O1	1.857(5)
V1-O2	1.933(6)	V1-O2	1.959(4)
V1-O3	1.554(6)	V1-O3	1.582(5)
V1-O4	2.335(6)	V1-O4	2.266(5)
V1-O4^i	1.812(6)	V1-O5	1.762(5)
V1-N1	2.128(6)	V1-N1	2.132(5)
C8-O2	1.309(10)	C8-O2	1.299(8)
C8-N2	1.295(11)	C8-N2	1.293(9)
O1-V1-O2	150.2(3)	O1-V1-O2	150.6(2)
O1-V1-O3	100.8(3)	O1-V1-O3	101.5(2)
O1-V1-O4	81.6(3)	O1-V1-O4	81.5(2)
O1-V1-O4^i	104.3(3)	O1-V1-O5	100.8(2)
O1-V1-N1	82.0(3)	O1-V1-N1	82.4(2)
O2-V1-O3	100.0(3)	O2-V1-O3	97.9(2)
O2-V1-O4^i	91.6(3)	O2-V1-O4	77.9(2)
O2-V1-O4	78.9(2)	O2-V1-O5	96.9(2)
O2-V1-N1	74.6(2)	O2-V1-N1	74.4(2)
O3-V1-O4	175.9(3)	O3-V1-O4	174.9(2)
O3-V1-O4^i	102.5(3)	O3-V1-O5	101.1(3)
O3-V1-N1	96.9(3)	O3-V1-N1	93.7(2)
O4-V1-O4^i	73.7(3)	O4-V1-O5	82.3(2)
O4^i-V1-N1	157.9(3)	O4-V1-N1	82.4(2)
O4-V1-N1	86.5(2)	O5-V1-N1	163.8(2)

i = –x,1–y,1–z

Table 7

Oxidation of various hydrocarbons with **1**, **2**, **4**, **5**, **8** using H_2O_2 in acetonitrile.[a]

Entry	Substrate	Product (s)		Conv. (%)[b] /Yield (%)/Time (h) / TOF (h^{-1})[c]				
			Catalyst	**1**[d]	**2**[e]	**4**[e]	**5**	**8**[e]
1	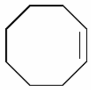	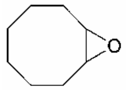	92	70	96	70	60	
				92	70	96	70	60
				5	5	4	4	3
				108	82	141	102	118
2	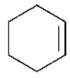	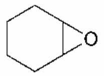		96	95	99	78	73
				15	15	50	60	41
				4	5	3	4	5
				142	112	194	114	86
		Yield (%) (2-Cyclohexen-1-ol)		45	19	46	14	30
		Yield (%) (2-Cyclohexen-1-one)		36	61	3	4	2
3	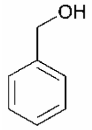	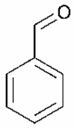		59	30	16	55	16
				59	30	16	55	16
				5	5	4	5	5
				70	36	24	64	18
4	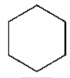	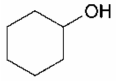		14	83	93	25	92
				14	83	93	25	92
				5	5	4	4	4
				16	98	137	36	136
5	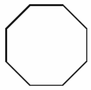	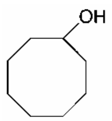	50	35	23	26	18	
				31	25	20	16	17
				4	5	5	5	5
				74	42	27	30	22
		Yield (%) (Cyclooctanone)		19	10	3	10	1

[a] Reaction conditions: catalyst 1.70 µmol, substrate 1 mmol, H_2O_2 3 mmol, internal standard (chlorobenzene) 0.1 g, CH_3CN 3 ml, reaction temperature 80 ºC.

---

[b] Conversions are based on the starting substrates.

[c] TOF: turnover frequency which is calculated by the expression [products]/([catalyst]× time) (h^{-1})

[d] reaction temperature 60 ºC.

[e] $NaHCO_3$ 0.25 mmol.

Table 8
Oxidation characteristics of cyclooctene and cyclohexane by different transition metal complexes

No.	Substrate to product	Conv. (%)	Selec. (%)	Time (h)	Oxidant/Catalyst	TOF (h^{-1})	Ref.
1	Cyclooctene to cyclooctene oxide	92	100	5	$H_2O_2/[\{VO_2\}_2(H_2L^1)]$	108	This work
2		70	100	4	$H_2O_2/[\{VO(CH_3O)(CH_3OH)\}_2(L^2)]$	102	This work
3		84	100	4.5	$TBHP/V^{IV}O(L^3)_2$ [a]	7	[40]
4		29	100	6	$H_2O_2/[V^VOL^4Cl]$ [b]	5	[41]
5		39	100	6	$H_2O_2/[V^VOL^5Cl]$ [c]	7	[41]
6	Cyclohexane to cyclohexanol (A) / cyclohexanone (K)	93	100	4	$H_2O_2/NaHCO_3/[TiO(H_3L^1)_2]$	137	This work
7		31	58% A 42% K	1	H_2O_2/acetic acid/ $[(Me_3tacn)Mn(O)_3Mn(Me_3tacn)](PF_6)_2$ [d]	640	[42]
8		73	23% A 77% K	3	$H_2O_2/MnSO_4/Me_3tacn$/Na-oxalate [d]	53	[43]
9		82	22% A 66% K	1.5-4.5	H_2O_2/acetic acid/$[LMn(\mu\text{-}O)_3MnL][PF_6]_2$ [d]	74-222	[44]

[a] TBHP = tert-butylhydroperoxide, L3 = N-salicylidin-2-chloroethylimine

[b] $L^4=Me_2NCH_2CH_2N(CH_2\text{-}2\text{-}O\text{-}3,5\text{-}C_6H_2{}^tBu_2)_2$

[c] $L^5= Me_2NCH_2CH(CH_3)N(CH_2\text{-}2\text{-}O\text{-}3,5\text{-}C_6H_2{}^tBu_2)_2$

[d] L = Me_3tacn =1,4,7-trimethyl-1,4,7-triazacyclononane

Graphical abstract (synopsis)

Eight bis-tridentate terephthalo- and oxalohydrazide complexes of V(V), Cu(II), Mn(II) and Ti(IV) were prepared and characterized. The compound V-terph was a one-dimensional coordination polymer. The complexes catalyzed oxidation of hydrocarbons using H_2O_2 with good to excellent conversions and high selectivity.

Graphical abstract (Picture)

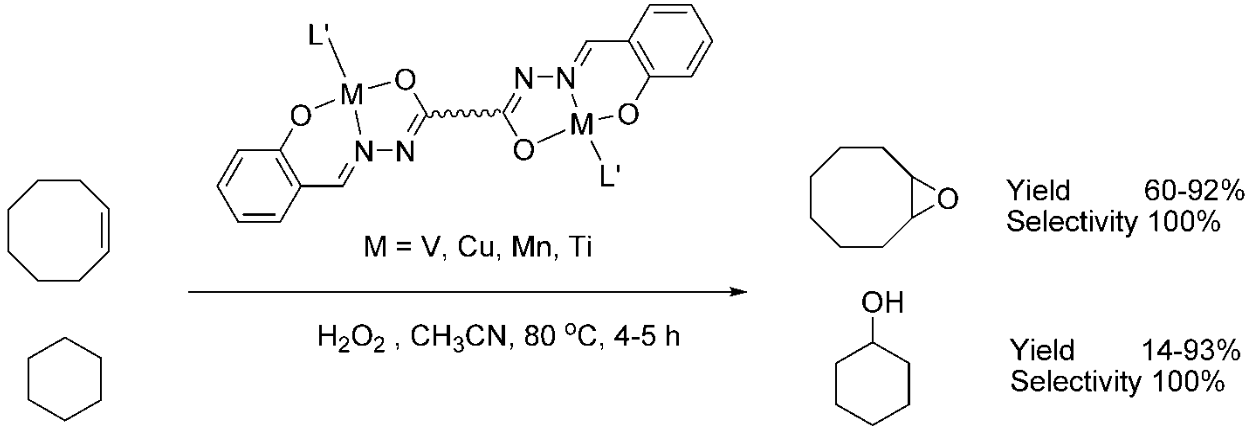

Highlights

- ✓ Eight new complexes of bis(aroyl)hydrazone are reported
- ✓ Crystal structures of one dinuclear and one 1D coordination polymer of V(V)-bis(aroyl)hydrazone are shown.
- ✓ The complexes show high catalytic activity and selectivity in the oxidations of various hydrocarbons with hydrogen peroxide.